



# HHS Public Access

Author manuscript

*Chem Commun (Camb)*. Author manuscript; available in PMC 2017 September 14.

Published in final edited form as:

*Chem Commun (Camb)*. 2008 October 21; (39): 4795–4797. doi:10.1039/b806685j.

## Spectrally tunable uncaging of biological stimuli from nanocapsules†

Kimberly A. Dendramis, Peter B. Allen, Philip J. Reid, and Daniel T. Chiu\*

Department of Chemistry, University of Washington, Seattle, WA 98195-1700, USA

### Abstract

This communication describes the first uncaging of stimuli in the far red, wavelengths that have much less of an adverse affect on cellular systems, *via* photolysis of photosensitized nanocapsules.

Biological cells exhibit complex spatial and temporal organization. To study the dynamic properties of cellular function, it is often necessary to apply spatiotemporally defined biochemical perturbations. Techniques capable of providing such perturbations are limited, and much effort has been spent to develop this capability. The most notable and promising of these methods is the photolysis of photoactivable or “caged” molecules,<sup>1–7</sup> as recently demonstrated in the mapping of the distribution of receptors and ion channels on the membrane, calcium fluxes in cells, and activity of neural circuits.<sup>1,7,8</sup> The applicability of caged compounds to biological studies is limited by the requirement of UV photoactivation for existing compounds,<sup>1–7</sup> because UV light can induce cellular damage, and this wavelength region has low tissue-penetration depths. This issue is partially overcome with two-photon uncaging, although two-photon photolysis still occurs in the UV region. The current selection of two-photon caged molecules, however, are limited and their absorption cross section is typically quite small (*e.g.* ~1 Goeppert–Mayer (GM)) in comparison to currently available two-photon chromophores (up to hundreds to thousands of GMs).

To address these issues, we report here the first one-photon uncaging of a physically caged stimulus in the far red, a wavelength region that provides for limited cellular damage and increased penetration depth, thereby increasing the utility of caged compounds in biological studies. Based on the same strategy of photosensitizing the shell of nanocapsules with chromophores, we also demonstrate the two-photon triggered release of stimuli and cellular activation.

Our strategy is based on the use of nanocapsules, which offer an attractive platform in which to develop “caged” molecules because traditional chemically caged compounds can be challenging to design and synthesize, often have low photolytic efficiency, and can be difficult to use in the caging of larger molecules such as bioactive peptides and proteins. Additionally, some caged compounds (*e.g.* carboxylic esters) may exhibit background biological activity due to dark hydrolysis. In contrast, nanocapsules based on physical cages

†Electronic supplementary information (ESI) available: Detailed experimental procedures. See DOI: 10.1039/b806685j  
chiu@chem.washington.edu; Fax: +1 206 685 8665; Tel: +1 206 543 1655.

can be applied to a wide range of bioactive molecules, and have high photolytic efficiencies<sup>9</sup> and fast uncaging times.<sup>10</sup> Background biological activity is readily controlled and eliminated by isolating the nanocapsules from the bioactive molecules that leaked from the capsules with size-exclusion chromatography. Alternatively, leakage from nanocapsules can be prevented by further “sealing” off the shell of the capsule (e.g. with polyelectrolytes and silica).<sup>12</sup> Our past work relies on the UV photolysis of nanocapsules.<sup>9–13</sup> Here, we describe our strategy to tune the photolysis wavelength by doping the shell of nanocapsules with highly absorptive chromophores.

Fig. 1(A) schematically illustrates our experimental setup and strategy, in which photolysis of the dye-sensitized nanocapsule effectively releases the encapsulated contents (inset). In our experiments, two lasers were employed, one for visualization (*via* epi-fluorescence) and the other for vesicle photolysis. For one-photon experiments, a blue solid-state laser (488 nm) was used for imaging and a nanosecond pulsed N<sub>2</sub> laser was used to pump a dye head attachment to generate laser pulses of a desired wavelength (645 nm). For the two-photon experiments, a green laser (532 nm) was used for visualization and a tunable mode locked Ti:Sapphire laser was used as a femtosecond pulsed light source. In our proof-of-concept experiments described here, lipid vesicles were used as nanocapsules given their ease of preparation; however a range of materials including silica and polymers can be employed.<sup>11,12</sup>

Fig. 1(B) shows the two-photon triggered release of carbachol from a vesicle (arrow) onto a Chinese hamster ovary cell that has been transfected to express the M1 acetylcholine receptor (CHO-M1 cell) and has been loaded with the calcium indicator Rhod2. We doped the membrane shell of the vesicle with DiI, which is readily excited at 532 nm for visualization and also has a strong two-photon absorption cross section near 710 nm (~100 GM at 700 nm).<sup>14</sup> In our previous work that relied on one-photon UV photolysis of nanocapsules, we had to position the vesicle using optical trapping to avoid UV damage to the cell. Here, no optical trapping was used and the vesicles were randomly distributed and non-specifically attached to the cell. Prior to photolysis (time 0 ms) intracellular calcium level was low and the cell was barely visible under fluorescence. After photolysis and uncaging of the encapsulated carbachol, intracellular calcium increased and propagated across the cell.

Although two-photon photolysis offers a true three-dimensional focal volume and high depth discrimination, photolysis nevertheless still occurs in the UV within the focal volume. Therefore, we decided to demonstrate one-photon uncaging in the far red where cellular absorption is near a minimum. We think one-photon far-red uncaging will be particularly useful for cell-culture samples, and given its ease of implementation in comparison to two-photon photolysis, may also find broad use in applications that involve organotypic cultures.

Our one-photon experiments used DiD, because of its high absorption cross section and ease of incorporation into the vesicle membrane. Fig. 2(A) shows the emission spectrum of the laser dye employed (DCM) to produce nanosecond (~3 ns) pulses of 645 nm light. The emission of DCM has excellent spectral overlap with the absorption of DiD. Fig. 2(B) depicts the “uncaging” of a 400 nm-diameter vesicle, which was doped with 13 mol% DiD,

with a single nanosecond pulse. For fluorescence visualization, carboxyfluorescein was encapsulated within the vesicle. Upon photolysis, the encapsulated dye molecules were released from the vesicle and then rapidly diffused away from the point of photolysis. The use of 400 nm capsules was motivated by the need to encapsulate a sufficient amount of dye to facilitate visualization, but smaller vesicles (*e.g.* 40 nm) also can be prepared easily with extrusion or sonication.<sup>9,11,12</sup> With other substrates and preparation methods, even smaller nanocapsules (*e.g.* 20 nm) should be possible.

Fig. 2(C) illustrates the advantages of using 645 nm laser pulses rather than UV (355 nm) laser pulses for uncaging. The figure shows the response of CHO cells after being hit by a single nanosecond laser pulse at the respective wavelengths (note that no vesicles are present in these experiments). For readout of cellular response, calcium imaging was employed by loading the cell with Fluo3, a calcium sensitive dye readily excited at 488 nm. Calcium mediates signaling pathways for cellular repair and apoptosis,<sup>15</sup> and thus its level acts as a reporter of cell stress. Fig. 2(C) presents a histogram of cell response to a single laser pulse. We did not observe any cellular response (*i.e.* increase in intracellular levels of calcium) to 645 nm laser pulses, tested at the highest pulse energy required to photolyze our vesicles (560 nJ). In contrast, 355 nm UV laser pulses readily elicit cellular response and cause cell stress, with increasing number of cells responding as the pulse energy was increased from 80 to 380 nJ to 780 nJ. Next, we applied our method to achieve spatiotemporally resolved stimulation of single cells (Fig. 2(D) and (E)). In Fig. 2(D), the vesicles were loaded with bradykinin, a peptide containing nine amino acids; the response of rat PC12 cells was studied as our model system. The PC12 cells were grown on collagen coated glass coverslips and given nerve growth factor (NGF) to promote the formation of neurites. The first panel of Fig. 2(D) contains two PC12 cells growing adjacent to each other; only the outlined cell was activated. When bradykinin binds to the B<sub>2</sub> receptor, hydrolysis of PtdInsP<sub>2</sub> and formation of Ins(1,4,5)P<sub>3</sub> occurs, resulting in the increase of intracellular Ca<sup>2+</sup>, which we can visualize with our calcium indicator dye Fluo3.<sup>16</sup> The responses of PC12 cells to bradykinin were generally less prominent than the responses elicited of CHO-M1 cells with carbachol. Fig. 2(E) is an additional example of one-photon photolysis. Here the vesicle was loaded with carbachol to activate a CHO-M1 cell and shows a much brighter response than the PC12 cell.

Appropriate doping of the shell of nanocapsules with highly absorptive chromophores offers a versatile and convenient path to tune the photolysis wavelengths and properties of nanocapsules. This communication demonstrates and validates this strategy; future work will focus on determining the mechanism of photolysis in order to design more robust and biocompatible nanocapsules using the most suitable starting nanomaterial, such as block copolymers conjugated with the desired chromophore. For example, DiI has a two-photon absorption cross section of ~100 GM, but two-photon chromophores with much higher absorption cross sections (thousands of GMs) have been synthesized and may be employed. Once developed, such nanocapsules can be used to cage a wide range of molecules of interest, from small molecules and ions to DNAs, proteins, and peptides. This feature contrasts with the need to synthesize and tune new photosensitive chemical groups and linkage chemistries each time a new chemically caged molecule is to be developed. The ability to uncage a wide range of bioactive molecules in the far red or near infrared will be

particularly beneficial for intracellular and *in vivo* applications, and we believe such capability will find broad use in studies that probe the complex organization of the cell.

## Supplementary Material

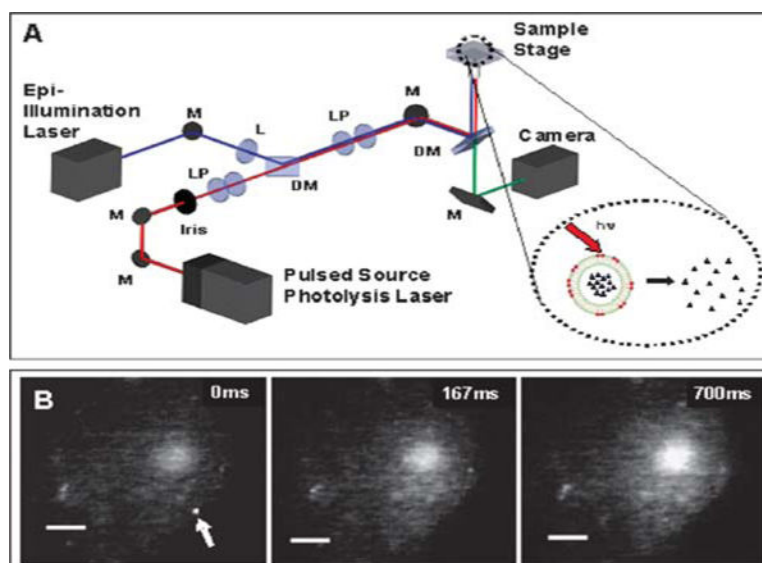
Refer to Web version on PubMed Central for supplementary material.

## Acknowledgments

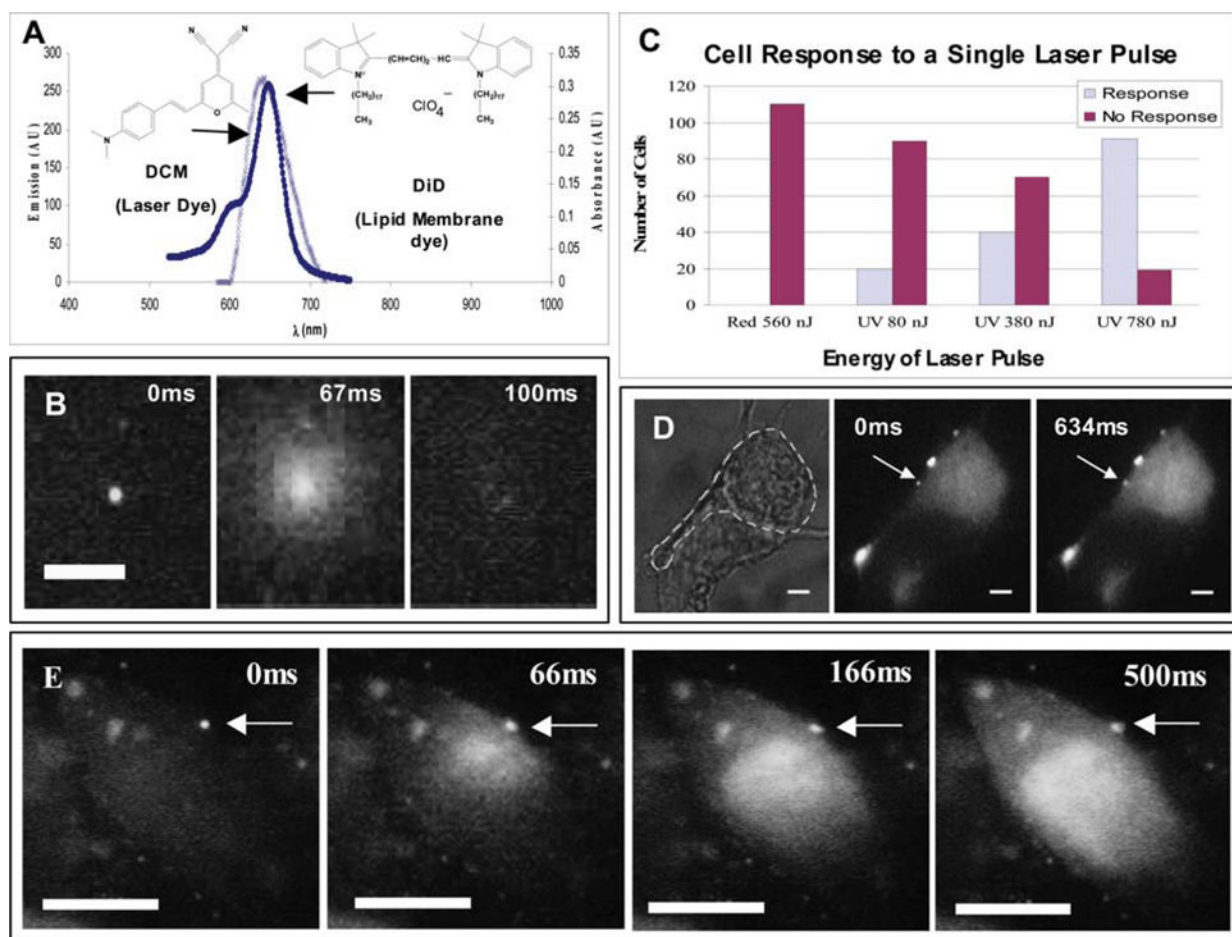
K. A. Dendramis acknowledges support from the Center of Nanotechnology at the University of Washington for a UIF and IGERT fellowship. The authors are grateful to NIH (AG 029574) and the McKnight Foundation for support of this work.

## Notes and references

1. Pettit DL, Wang SS, Gee KR, Augustine GJ. *Neuron*. 1997; 19:465–471. [PubMed: 9331338]
2. Adams DR, Tsien RY. *Annu Rev Physiol*. 1993; 55:755–784. [PubMed: 8466191]
3. Li WH. *Nat Methods*. 2006; 3:13–15. [PubMed: 16369546]
4. Furuta T, Wang SSH, Dantzker JL, Dore TM, Bybee WJ, Callaway EM, Denk W, Tsien RY. *Proc Natl Acad Sci U S A*. 1999; 96:1193–1200. [PubMed: 9990000]
5. Zhao Y, Zheng Q, Dakin K, Xu K, Martinex ML, Li WH. *J Am Chem Soc*. 2004; 126:4653–4663. [PubMed: 15070382]
6. Momotake A, Lindegger N, Niggli E, Barsotti RJ, Ellis-Davies GCR. *Nat Methods*. 2006; 3:35–40. [PubMed: 16369551]
7. Li WH, Llopis J, Whitney M, Zlokarnik G, Tsien RY. *Nature*. 1998; 392:936–941. [PubMed: 9582076]
8. Nikolenko V, Poskanzer KE, Yuste R. *Nat Methods*. 2007; 4:943–950. [PubMed: 17965719]
9. Sun BY, Chiu DT. *J Am Chem Soc*. 2003; 125:3702–3703. [PubMed: 12656592]
10. Sun BY, Lim DSW, Kuo JS, Kuyper CL, Chiu DT. *Langmuir*. 2004; 20:9437–9440. [PubMed: 15491172]
11. Sun BY, Chiu DT. *Langmuir*. 2004; 20:4614–4620. [PubMed: 15969173]
12. Sun BY, Mutch SA, Lorenz RM, Chiu DT. *Langmuir*. 2005; 21:10763–10769. [PubMed: 16262349]
13. Sun BY, Chiu DT. *Anal Chem*. 2005; 77:2770–2776. [PubMed: 15859592]
14. Xu C, Webb WW. *J Opt Soc Am B*. 1996; 13:481–491.
15. Berridge MJ, Bootman MD, Lipp P. *Nature*. 1998; 395:645–648. [PubMed: 9790183]
16. Fasolato C, Pizzo P, Possan T. *J Biol Chem*. 1990; 265:20351–20355. [PubMed: 2122973]



**Fig. 1.** (A) Schematic of experimental setup. (B) A sequence of images showing the response of a CHO-M1 cell loaded with Rhod2 to the two-photon triggered release of carbachol from a single 400 nm diameter vesicle (arrow). The vesicle membrane was doped with DiI at 2.5 mol%, and was photolyzed with a 8 ms pulse train from a Ti:Sapphire laser (710 nm; 120 fs pulses at 80 MHz; 40 mW of average power). The first panel was recorded just prior to application of the laser pulses. Vesicles were formed by extrusion in PBS (phosphate-buffered saline; pH = 7.5) that contained 1 mM carbachol; non-encapsulated molecules were removed by passing the sample twice through a size-exclusion column (Sephacryl 100, Amersham Bio-sciences). The scale bars are 3  $\mu\text{m}$  and the  $z$ -scale remains the same throughout.

**Fig. 2.**

(A) Spectra showing the overlap of the emission spectrum of the laser dye, DCM, with the absorbance spectrum of the membrane dye, DiD. (B) A sequence of images showing the photolysis of a single 400 nm-diameter vesicle, which was loaded with ~50 mM carboxyfluorescein. The vesicle was photolyzed using a single ~3 ns pulse from the 645 nm output of a  $N_2$ -pumped dye laser. Vesicles were formed by extrusion and underwent three freeze–thaw cycles to increase encapsulation efficiency. (C) A histogram showing the response of cells after being hit by a single UV (355 nm) or red (645 nm) laser pulse at different energies (note that no vesicles were present in these experiments). Reported energies were measured just prior to the laser pulse entering a 100 $\times$  superfluor objective (NA = 1.3). (D) A sequence of images showing the response of a single PC12 cell loaded with Fluo3 to the release of bradykinin from a single vesicle using a single ~3 ns pulse at 645 nm. The vesicle was doped with DiD and DiO C-18 at 13 and 1 mol%, respectively. DiO C-18 (excited at 488 nm) was used to visualize the vesicles under epi-fluorescence imaging. The first panel is a brightfield image of two overlapping PC12 cells; the cell to be activated is outlined. The second panel was recorded just before application of the laser pulse. Vesicles were formed by extrusion in PBS (phosphate-buffered saline; pH = 7.5) containing 500 nM bradykinin. (E) A sequence of images showing the response of a CHO-M1 cell loaded with Fluo3 to the release of carbachol from a single vesicle. The vesicle was

doped with DiD and DiO C-18 at 13 and 1 mol%, respectively. The first panel was recorded just before application of the laser pulse. Vesicles were formed by extrusion in PBS containing 1 mM carbachol. All scale bars are 3  $\mu\text{m}$  and the  $z$ -scale remains the same throughout.

Author Manuscript

Author Manuscript

Author Manuscript

Author Manuscript